Integration of a High Frequency Inductive Power Transfer System to Energize Agricultural Sensors Through Soil

John Sanchez*, Juan M. Arteaga†, Cody Zeisiger‡, Darrin J. Young§, Ramesh Goel¶, Paul D. Mitcheson†, Eric M. Yeatman† and Shad Roundy*

*Department of Mechanical Engineering, The University of Utah, Salt Lake City, Utah, USA,
†Department of Electrical and Electronic Engineering, Imperial College London, London, UK,
‡Utah State University, Ogden, Utah, USA,
§Department of Electrical and Computer Engineering, University of Utah, Salt Lake City, Utah, USA,
¶Department of Civil and Environmental Engineering, University of Utah, Salt Lake City, Utah, USA.

2022 Wireless Power Week (WPW) | 978-1-6654-8445-9/22/$31.00 ©2022 IEEE | DOI: 10.1109/WPW54272.2022.9853990

***Abstract*—This paper describes the design and integration of a 13.56 MHz inductive power transfer (IPT) system and an in-house underground soil sensor network. The transmitter of this wireless power system was retrofitted on a Matrice 100 drone for periodic fast-charging missions, and the receiver was designed to fit into a sealed underground enclosure. The experiments reported in this paper involve a 40-day agricultural field trial where power was fed wirelessly to the soil sensor network. During this trial, the receiver's enclosure was buried at a depth of 200 mm in soil. These experiments feature an average charging efficiency (from the drone's battery to the underground station) of 33.5% (5% peak) with a peak power transfer of 35 W. Compared to laboratory testing, a significant increase in the end-to-end losses (of around 30 W) was observed in the field tests due to the presence of soil.**

The work reported in this paper is part of a collaborative project which looks to enable state-of-the-art high-frequency wireless power technology in agricultural applications.

***Index Terms*—High Frequency Inductive Power Transfer, Soil Moisture Sensor, Underground Sensors, Underground Power Transfer.**

I. Introduction

Historic droughts and changes in water management policy have led to a drastic shift in how the agricultural sector uses water and technology [1]. Agricultural soil sensors can support water conservation by helping farmers better control irrigation in their fields. While useful, these sensors often rely on above-ground hardware (solar panels, telemetry systems, etc.) that is obtrusive to farmers and easily damaged by inclement weather, farm equipment, and livestock. One proposed solution to the issues with above-ground installations is to bury the entire soil monitoring system underground. However, a significant problem with entirely underground sensor networks is power management. For such a system to be effective, farmers must be able to power their hardware without needing to excavate the entire system and replace its batteries periodically.

The following work presents a collaborative effort between the University of Utah, Imperial College London, the University of Aberdeen, and Utah State University to create an effective *in-situ* soil monitoring system. Our underground sensor network is recharged entirely by high-frequency inductive power transfer (HF-IPT) through the soil. Our power management system eliminates the need for semi-permanent above-ground hardware and periodic battery replacement. This work's wireless power transfer system expands on our previous research [2]–[4].

II. Design and Construction of the Soil Sensor

The Utah Soil Sensor (Fig. 1.a) was designed to be accurate and compatible with our HF-IPT system. Like most soil moisture sensors, this custom sensor operates by measuring changes in a sample's permittivity. Soil moisture sensors often rely on measuring this parameter because the permittivity of water ($\epsilon_r \approx 80$) is significantly larger than that of dry minerals ($\epsilon_r \approx 6$) and dominates the measured dielectric constant of soil. Our sensor indirectly measures relative permittivity by measuring frequency shifts in an RCL oscillator circuit.

Prior works have demonstrated that this custom sensor performs nearly as accurately as commercially available soil sensors while significantly reducing power consumption during active use [5]. Commercial sensors such as the Acclima TDR-310H and Delta-T ML3 ThetaProbe typically boast accuracy levels of 1-2% (0.01-0.02 $cm^3 \cdot cm^{-3}$) [6] [7]. This custom soil sensor reports soil moisture content with an accuracy of 1.75% (0.0175 $cm^3 \cdot cm^{-3}$) for sandy and loamy soils. The most recent iteration of this custom sensor consumes less than 2.97 mJ (3.3 V, 6 mA, 150 ms conversion time) per moisture measurement. This energy benchmark is at minimum 26.9x times less than the TDR-310H (80-120 mJ) [6] and 15.15x less than the ML3 ThetaProbe (45-252 mJ) [7]. These low-energy characteristics make this custom soil sensor ideal for situations with intermittent charging and no easy user access.

III. Design of the HF-IPT System for Wireless Power Transmission Through Soil

The HF-IPT system was explicitly designed to transmit power wirelessly from a drone-mounted coil to an underground sensor installation. We designed the transmitter to fit beneath a

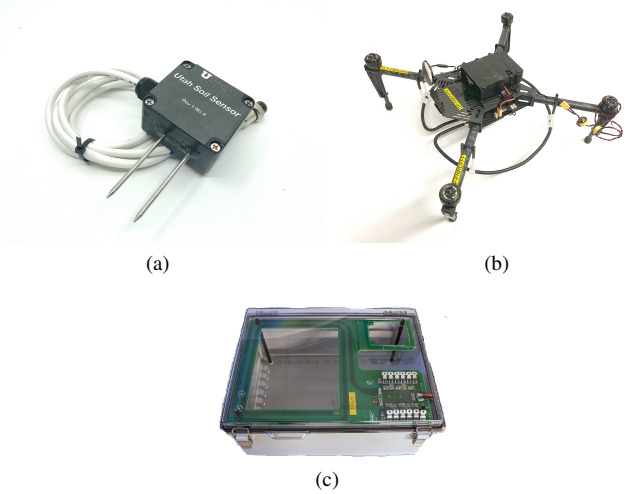

(a) (b)

(c)

Fig. 1. Equipment photographs: (a) Utah Soil Sensor, (b) Matrice 100 drone with an HF-IPT transmitter, and (c) IP67 enclosure with an HF-IPT receiver.

DJI Matrice 100 drone (Fig. 1.b). This drone's battery (TB47D by DJI; 4500 mAh; 22.2 V) provides the 13.56 MHz HF-IPT system with power. This frequency is the ISM band optimal for the size of the coils. The transmitter features a single-turn 10 mm diameter, 0.9 mm wall-thickness copper-pipe coil with a 200 mm radius. Meanwhile, our coupled receiver uses a PCB coil mounted inside a waterproof plastic enclosure (Fig. 1.c). We selected a relatively large IP67 plastic enclosure (255 mm x 130 mm x 80 mm) to contain the coil and additional electronics. The coupling factor we measured from transmitter to receiver coil was between 3 and 5%, corresponding to an air gap of 250 to 320 mm and lateral coil misalignment lower than 100 mm.

A. Transmit and Receive Coil Drivers

The inverter of the HF-IPT transmitter is a load-independent [8] Class EF inverter (Fig. 2.a), which is a proven topology and tuning method for applications with variable coupling and a variable load [9]. The receiver uses a Class D (Fig. 2.b) voltage multiplier rectifier to drive the hardware inside the underground station from a relatively low induced voltage on the receive coil. Our prior works present experiments using these transmitter/receiver topologies [2].

B. Supercapacitor Module for Fast Charging

The HF-IPT receiver outputs a voltage of 120 to 240 V, which feeds two off-the-shelf converters: a 42 V battery/supercapacitor charger (configured to output 825 mA) and an off-the-shelf 5 V converter to power a Bluetooth LE module. This battery charger features a voltage protection circuit that slows down power conversion under approximately 15.5 to 20 V. The 42 V charger energizes twenty 200 F supercapacitors (SSC-Series by AVX) in series from 20 to 42 V (from 22.7 to 100% charge) in under five minutes. The Bluetooth LE module [10] was integrated to monitor the receiver of the HF-IPT system remotely and in real-time. This

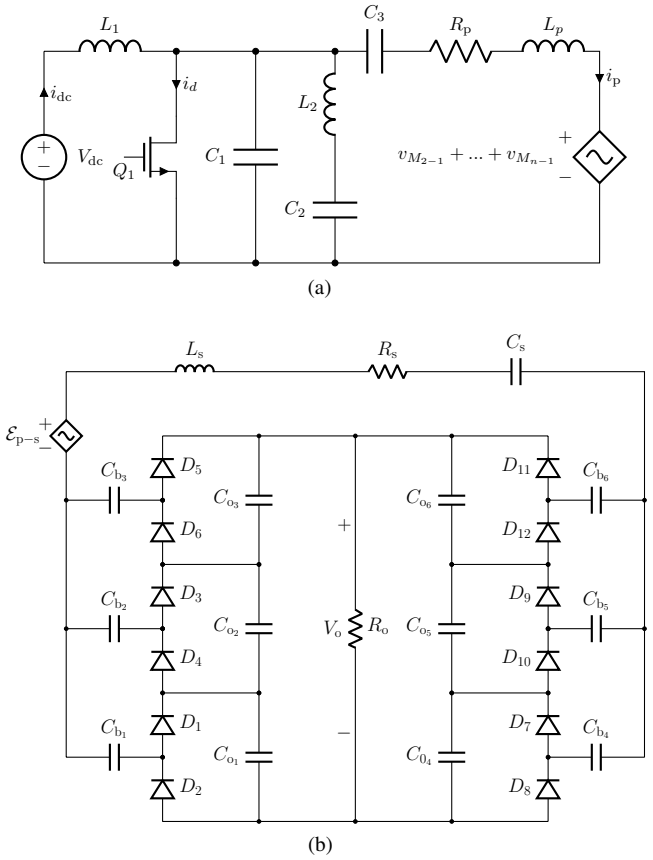

Fig. 2. Circuit schematics: (a) Class EF inverter and (b) voltage tripler Class D rectifier.

module uses the independent 5 V supply since it is active only when power is fed into the underground HF-IPT receiver.

IV. Design and Construction of a Sensor Network for Data and Energy Storage

The receiver's supercapacitor bank acts as the energy storage stage linking the wireless power transfer system to the sensor network. We implemented a DC/DC step-down converter to step down the supercapacitor bank's variable voltage (0-42 V) to 5 V with an efficiency of approximately 80% at 42 V [11]. Our remaining underground electronics are configurable and can operate solely from this 5 V rail or in conjunction with a lithium battery and corresponding charger circuit.

Data are stored in the underground station on a 32 GB SD card using an ATSAMD21G18 evaluation board [12]. This board also communicates with several peripherals, such as a real-time counter (RTC) module and up to three Utah Soil Sensors. Two 10-bit analog-to-digital converters on this microcontroller measure the voltage of the supercapacitor bank and the HF-IPT system's rectifier circuit. Both voltages are obtained using simple resistive dividers and several bypass capacitors. Our evaluation board also communicates directly to the Bluetooth LE module, which is used to monitor the state of the HF-IPT receiver in real-time.

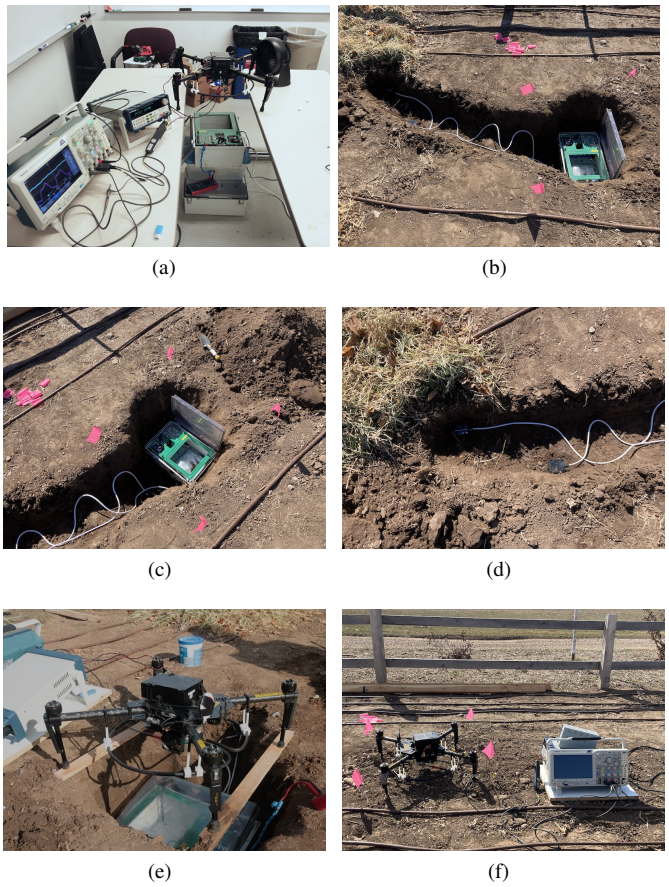

Fig. 3. Photographs of the HF-IPT experiments: (a) laboratory setup, (b) field setup, (c) buried WPT enclosure, (d) buried sensors, (e) uncovered experiment, and (f) covered experiment.

V. HF-IPT Laboratory Experiment Results

Our prior work presents benchmark figures of our HF-IPT configuration [2]. During those tests, we delivered a maximum power of 16.5 W to the bank of supercapacitors. With slight adjustments to the tuning, we have increased the received power to 35 W. Our laboratory setup (Fig. 3.a) showed better peak efficiency (50.6%) than in the field (33.5%). Both experiments used a coil-to-coil gap of 290 mm. In our field tests, 200 mm of this gap contained soil. These efficiency figures are calculated for the voltage range of 15.5 to 42 V, roughly when the battery charger's under-voltage protection circuit (slows down charging) is disabled. Table I summarizes the results from our laboratory and field experiments.

VI. Field Experiment Setup

We tested the combined HF-IPT/sensor system at the Utah State University Botanical Center in Davis County, Utah. This site is used for conducting agricultural research and contains several testbeds with arable soil and live plants. Our team buried the underground station 200 mm underground near a dormant carnation flower (*Dianthus caryophyllus*) testbed. The bulk density of the soil above the receiver station was 1.01 $g \cdot cm^{-3}$ (measured by dry baking and weighing a 937.8 cm^3 core sample). This low bulk density indicates that soil was loosely packed above the receiver. We connected two soil sensors to this station: one adjacent to the flower testbed and another 0.5 m away from the testbed.

TABLE I
Summary of the HF-IPT Results

Variable	Laboratory (air)	Field (air + soil)
Maximum Receiver Power	34.7 W	34.7 W
Maximum Transmitter Power	62.9 W	92.9 W
Total Receiver Energy	7.62 kJ	7.62 kJ
Total Transmitter Energy	15.05 kJ	22.78 kJ
Transmission Energy Efficiency	50.6 %	33.5 %

Before being buried, we placed a fully charged lithium battery (single cell, 2200 mAhr) inside the receiver station. This battery was used as a backup to prevent potential losses of data. While this battery is the primary energy source for the underground hardware, the supercapacitor bank charges the battery during each recharge event. We configured our evaluation board to log data every ten seconds. While soil moisture generally does not change appreciably in such a short amount of time, this period helped stress our system and collect meaningful power transfer data. At this fast data logging rate, the entire soil monitoring system uses an average of 1 mA at 3.3 V (reverts to sleep mode between measurements). With this current draw, the supercapacitor bank could realistically power the sensors for 12 hrs. However, this data rate is faster than necessary and hourly measurements (more than adequate for soil monitoring) would reduce the system's power consumption to 0.1 mA. At this more realistic current draw, the system can survive for roughly five days before needing a recharge. After a final inspection, the station was covered in soil and charged using the HF-IPT transmitter. We left the receiver underground for 40 days, starting on February 10, 2022, and ending on March 22, 2022.

A research team member provided power to the underground station every ten days using the HF-IPT transmitter attached to the Matrice drone. After each recharge, the underground station was partially excavated to verify that our hardware was working as expected. Note that we delayed the HF-IPT recharge scheduled for the 30th day of experimentation by several days due to snowfall and frozen conditions in Kaysville, Utah (Fig. 5.b and Fig. 5.d).

VII. Field Experiment Results

Our HF-IPT transmitter successfully charged the supercapacitor bank throughout the entire experiment. Fig. 4.a shows the supercapacitor's voltage and power as a function of time for the whole trial. On average, each charge cycle energized the supercapacitors to 8.61 kJ, or 97.6% of the energy anticipated for a 10 F capacitor bank at 42 V. In these figures, we observe numerous periods of time for which our underground equipment did not store any data. This loss of data is further discussed in *Section VIII* of this paper.

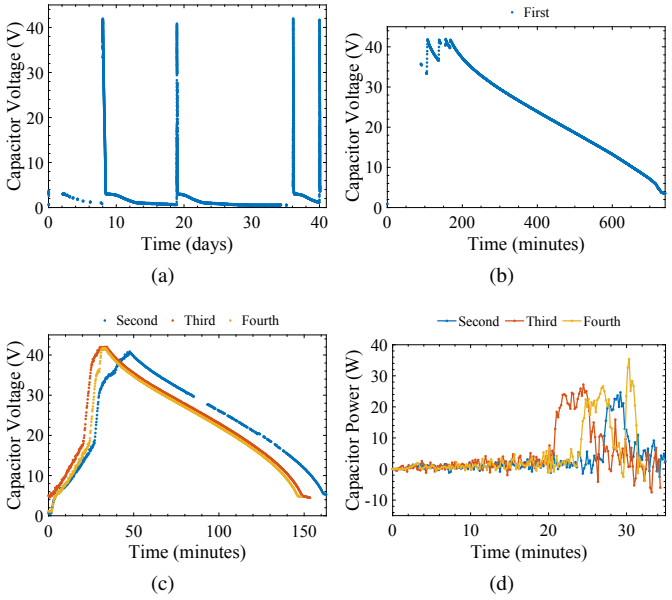

Fig. 4. Supercapacitor data: (a) full voltage history, (b) 1st recharge/discharge, (c) 2nd, 3rd, and 4th recharges/discharges, and (d) supercapacitor power during recharges.

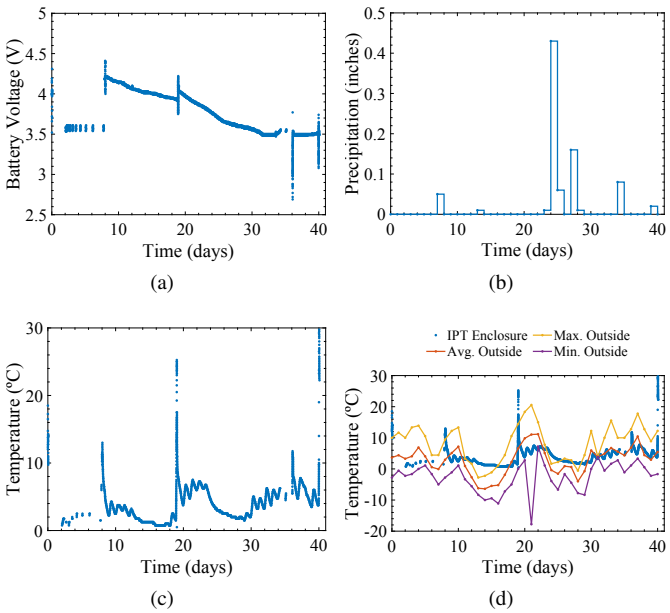

Fig. 5. Additional data: (a) lithium battery voltage, (b) average precipitation [13], (c) HF-IPT enclosure temperature, and (d) above-ground temperature [13].

Our first recharge cycle (requiring charging from 0-42 V) took approximately 100 minutes to complete (Fig. 4.b). Part of the data of this charge is missing due to inactivity in the underground station. The remaining three recharges took, on average, 30 minutes (Fig. 4.c). Our first recharge cycle took significantly longer because we initially misplaced the drone. This misplacement resulted in reduced coupling and, therefore, slower power transfer (the under-voltage protection system of the charger would be triggered when the charger increases the load). Similarly, the first cycle discharged slower because the lithium battery had a higher charge level at this point in time. Each cycle displayed in Fig. 4.c shows the four stages of our recharge cycle: slow initial charging (0 to 18 V), fast charging (18 to 42 V), battery charging, and long-term discharging. The initial slow stage occurs because the charger operates in current pulse-mode as opposed to constant-current mode as a precaution at low voltage. After this period of slow charging is finished, the battery charger is able to energize the capacitors from 20-42 V in 5-10 minutes (depending on whether the under-voltage protection system was triggered). The battery charging stage of this cycle occurs when the supercapacitor bank reaches full charge and begins to charge the lithium battery in the underground station. The final stage of the cycle occurs once the supercapacitor bank discharges to 5 V. Below this voltage, the lithium battery charger ceases to work, and the supercapacitors slowly discharge over several days.

Fig. 4.d shows the input power to the supercapacitor bank during the first two stages of our charging cycles. These data were obtained by calculating the energy stored in the supercapacitor bank over time and then taking the derivative. We observe that the average input power to the supercapacitor bank during the slow stage of charging is roughly 3.5 W. During the fast charging stage, the peak power increased to approximately 29.1 W (average for all three cycles; 35.4 W peak between all cycles).

During the entire course of experimentation, the lithium battery's voltage never fell under its nominal voltage of 3.5 V (Fig. 5.a). Note that these data cannot be used to accurately calculate battery charge, given the large variability in enclosure temperature. From the data shown in Fig. 5.a, we observed that the HF-IPT induced voltages in the cables connected to our battery caused extraneous voltage measurements. Despite temperatures in Kaysville swinging to 0°C and below (Fig. 5.d), the receiver station was deep enough to avoid freezing (Fig. 5.c). The temperature spikes seen in Fig. 5.c are due to the process of partially excavating the receiver and exposing it to sunlight.

Our system successfully collected soil data during the experiment. Throughout testing, we measured moisture values ranging from 12 to 22% by volume. However, in addition to the intermittent data gaps shown in Fig. 4-5, there were several additional periods for which the sensors were inactive for longer amounts of time. On most days, the sensors collected data for several hours. Therefore, the range of moisture values we collected may not accurately reflect moisture trends for the entirety of the 40-day experiment. This additional loss of data is further discussed in *Section VIII* of this paper.

VIII. Field Trial and System Integration Challenges

Throughout testing in the field, we faced challenges with the HF-IPT receiver, our sensor network, and the integration of the separately developed systems.

Fig. 6. Sensor connection points filled with dirt and moisture.

A. Localization

While the HF-IPT system is resistant to coil misalignment and was designed to operate at a relatively broad range in coupling, knowing where to place the drone with the required degree of precision during each recharge cycle proved challenging. This is exemplified by one of the recharging missions, which took over 100 minutes to fully charge the supercapacitor bank due to misplacement (Fig. 4.b). Our system explicitly seeks to avoid above-ground indicators; therefore, the implementation of automated, precise landing for drones would be required [14], [15].

B. Weatherproofing and Waterproofing

The transmission hardware mounted on the Matrice drone is a prototype that does not include a weather seal. Likewise, we do not intend to fly our drone missions in adverse weather conditions or freezing temperatures (as a safety measure for our batteries). These limitations caused significant delays in our testing schedule due to snowfall.

We observed a waterproofing issue with the underground receiver station. While the IP67 enclosure and each soil sensor are waterproof, their connections failed to perform as expected. Almost as soon as the receiver station was placed underground, the circular connectors used to communicate with the soil sensors filled with dirt and moisture (Fig. 6). We believe the soil and water in these connection points are responsible for the periodic data gaps visible throughout Fig. 4 and Fig. 5. Likewise, we believe that this connection point was responsible for the loss of moisture data intermittently throughout the experiment. Future iterations of the enclosure and attached sensors will avoid this issue by redesigning this connection point.

C. Electromagnetic Interference

While the electronics in our underground station generally performed as expected, we noticed some issues while the HF-IPT system was active. Despite our attempts to avoid placing wires near the receive coil, we could not move some of the cables without system-level redesigns. We observed significant EMI in most wires adjacent to the receive coil. While we expected to see EMI in our system, we observed several disruptive EMI effects in cables and PCB traces we did not anticipate being sensitive to EMI. Accordingly, integrating the Utah Soil Sensors with the data storage hardware proved challenging but overall improved the soil sensors and how they communicate with the receiver station. While communication protocols such as SPI and SDI-12 are popular in environmental monitoring sensors, they share data using single-ended signaling. Under the intense EMI caused by HF-IPT, these communication protocols failed to perform adequately in our tests and occasionally caused unpredictable errors in our sensors. Current iterations of the soil sensor communicate using RS-485 to address the issues we observed when using SPI and SDI-12. This protocol uses differential signaling and is far more resistant to EMI than our other protocols.

IX. Conclusions and Future Work

Our experiments demonstrate that power can successfully be transmitted from a drone-mounted coil to an underground soil sensor network. We measured a peak charge rate of 35 W and an efficiency of 33.5%. We were able to identify numerous logistic and technical challenges with full-system integration. Future iterations of the drone transmitter and underground sensor network will be designed to address the difficulties of full-system integration.

Acknowledgement

The authors would like to acknowledge the following funding sources: SitS NSF-UKRI, Wireless In-Situ Soil Sensing Network for Future Sustainable Agriculture.

References

[1] C. Becerra-Castro, "Wastewater reuse in irrigation: a microbiological perspective on implications in soil fertility and human and environmental health," *Environment International*, vol. 75, p. 117, 2014.

[2] J. M. Arteaga, P. D. Mitcheson, and E. Yeatman, "Development of a fast-charging platform for buried sensors using high frequency ipt for agricultural applications," in *2022 IEEE Applied Power Electronics Conference and Exposition (APEC)*. IEEE, 2022.

[3] P. D. Mitcheson, D. Boyle, G. Kkelis, D. Yates, J. A. Saenz, S. Aldhaher, and E. Yeatman, "Energy-autonomous sensing systems using drones," in *2017 IEEE SENSORS*. IEEE, 2017, pp. 1–3.

[4] J. M. Arteaga, S. Aldhaher, G. Kkelis, C. Kwan, D. C. Yates, and P. D. Mitcheson, "Dynamic capabilities of multi-MHz inductive power transfer systems demonstrated with batteryless drones," *IEEE Trans. on Power Electron.*, vol. 34, no. 6, pp. 5093–5104, June 2019.

[5] J. Sanchez, A. Dahal, C. Zesiger, R. Goel, D. Young, and S. Roundy, "Design and characterisation of a low-power moisture sensor from commercially available electronics," in *IEEE SENSORS Proceedings*, 2021, pp. 1–4.

[6] *True TDR-310H soil water-temperature-BEC sensor datasheet*, Acclima, Inc., 2019.

[7] *User Manual for the ML3 ThetaProbe*, Delta-T Devices Ltd., 2017.

[8] S. Aldhaher, D. C. Yates, and P. D. Mitcheson, "Load-independent class E/EF inverters and rectifiers for MHz-switching applications," *IEEE Trans. on Power Electron.*, pp. 1–1, 2018.

[9] J. M. Arteaga, S. Aldhaher, G. Kkelis, D. C. Yates, and P. D. Mitcheson, "Multi-MHz IPT systems for variable coupling," *IEEE Trans. on Power Electron.*, vol. 33, no. 9, pp. 7744–7758, Sept 2018.

[10] *Adafruit Feather M0 Bluefruit LE Overview*, Adafruit, 2016.

[11] *LM2593HV SIMPLE SWITCHER® power converter 150-kHz, 2-A step-down voltage regulator*, Texas Instruments, 2016, rev. SNVS082E.

[12] *Adafruit Feather M0 Adalogger Overview*, Adafruit, 2015.

[13] *Ogden-Hinckley Airport Station Weather History*, Weather Underground, 2022, https://www.wunderground.com.

[14] L. Lan, T. Polonelli, Y. Qin, N. Pucci, C. H. Kwan, J. M. Arteaga, D. Boyle, D. C. Yates, E. M. Yeatman, and P. D. Mitcheson, "An induction-based localisation technique for wirelessly charged drones," in *2020 IEEE PELS Workshop on Emerging Technologies: Wireless Power Transfer (WoW)*, 2020, pp. 275–277.

[15] Q. Qian, J. OKeeffe, Y. Wang, and D. Boyle, "Practical mission planning for optimized uav-sensor wireless recharging," *arXiv preprint arXiv:2203.04595*, 2022.